

# Fast switchable optical vortex generator based on blue phase liquid crystal fork grating

Shi-Jun Ge, Wei Ji, Guo-Xin Cui, Bing-Yan Wei, Wei Hu\* and Yan-Qing Lu

College of Engineering and Applied Sciences and National Laboratory of Solid State Microstructures, Nanjing University, Nanjing 210093, China  
\*huwei@nju.edu.cn

**Abstract:** Optical vortices have great potentials in optical communications, quantum computations, micro-manipulations and so on. At present, fast switching and reconfiguring of these beam vortices are still challenges. We proposed a blue phase liquid crystal fork grating by applying a vertical electric field with a forked electrode to the polymer stabilized blue phase liquid crystal cell. A fork shaped phase profile with alternation of isotropic and ordinary refractive indices in the lateral direction is thus obtained. Both fork gratings and fork grating array with different topological charges are demonstrated. They permit rapid optical vortex switching and topological charge tuning, and also exhibit excellent polarization independency and high efficiency.

©2014 Optical Society of America

**OCIS codes:** (230.3720) Liquid-crystal devices; (050.4865) Optical vortices; (050.0050) Diffraction and gratings; (110.3960) Microlithography.

---

## References and links

1. P. Couillet, L. Gil, and F. Rocca, "Optical vortices," *Opt. Commun.* **73**(5), 403–408 (1989).
2. J. P. Torres and L. Torner, *Twisted Photons: Applications of Light with Orbital Angular Momentum* (John Wiley & Sons, 2011).
3. A. M. Yao and M. J. Padgett, "Orbital angular momentum: origins, behavior and applications," *Adv. Opt. Photonics* **3**(2), 161–204 (2011).
4. L. Allen, M. W. Beijersbergen, R. J. Spreeuw, and J. P. Woerdman, "Orbital angular momentum of light and the transformation of Laguerre-Gaussian laser modes," *Phys. Rev. A* **45**(11), 8185–8189 (1992).
5. G. Foo, D. M. Palacios, and G. A. Swartzlander, Jr., "Optical vortex coronagraph," *Opt. Lett.* **30**(24), 3308–3310 (2005).
6. J. Wang, J. Y. Yang, I. M. Fazal, N. Ahmed, Y. Yan, H. Huang, Y. Ren, Y. Yue, S. Dolinar, M. Tur, and A. E. Willner, "Terabit free-space data transmission employing orbital angular momentum multiplexing," *Nat. Photonics* **6**(7), 488–496 (2012).
7. M. Beijersbergen, R. Coerwinkel, M. Kristensen, and J. Woerdman, "Helical-wavefront laser beams produced with a spiral phaseplate," *Opt. Commun.* **112**(5-6), 321–327 (1994).
8. X. C. Yuan, J. Lin, J. Bu, and R. E. Burge, "Achromatic design for the generation of optical vortices based on radial spiral phase plates," *Opt. Express* **16**(18), 13599–13605 (2008).
9. S. Slussarenko, A. Murauski, T. Du, V. Chigrinov, L. Marrucci, and E. Santamato, "Tunable liquid crystal q-plates with arbitrary topological charge," *Opt. Express* **19**(5), 4085–4090 (2011).
10. E. Brasselet and C. Loussert, "Electrically controlled topological defects in liquid crystals as tunable spin-orbit encoders for photons," *Opt. Lett.* **36**(5), 719–721 (2011).
11. E. Brasselet, N. Murazawa, H. Misawa, and S. Juodkazis, "Optical vortices from liquid crystal droplets," *Phys. Rev. Lett.* **103**(10), 103903 (2009).
12. Y. J. Liu, X. W. Sun, D. Luo, and Z. Raszewski, "Generating electrically tunable optical vortices by a liquid crystal cell with patterned electrode," *Appl. Phys. Lett.* **92**(10), 101114 (2008).
13. Y. J. Liu, X. W. Sun, Q. Wang, and D. Luo, "Electrically switchable optical vortex generated by a computer-generated hologram recorded in polymer-dispersed liquid crystals," *Opt. Express* **15**(25), 16645–16650 (2007).
14. M. Infusino, A. De Luca, V. Barna, R. Caputo, and C. Umeton, "Periodic and aperiodic liquid crystal-polymer composite structures realized via spatial light modulator direct holography," *Opt. Express* **20**(21), 23138–23143 (2012).
15. B. Y. Wei, W. Hu, Y. Ming, F. Xu, S. Rubin, J. G. Wang, V. Chigrinov, and Y. Q. Lu, "Generating switchable and reconfigurable optical vortices via photopatterning of liquid crystals," *Adv. Mater.* **26**(10), 1590–1595 (2014).

16. V. Y. Bazhenov, M. Vasnetsov, and M. Soskin, "Laser beams with screw dislocations in their wavefronts," *JETP Lett.* **52**, 429–431 (1990).
17. N. R. Heckenberg, R. McDuff, C. P. Smith, and A. G. White, "Generation of optical phase singularities by computer-generated holograms," *Opt. Lett.* **17**(3), 221–223 (1992).
18. I. C. Khoo and S. T. Wu, *Optics and Nonlinear Optics of Liquid Crystals* (World Scientific, 1993).
19. W. Hu, A. Srivastava, F. Xu, J. T. Sun, X. W. Lin, H. Q. Cui, V. Chigrinov, and Y. Q. Lu, "Liquid crystal gratings based on alternate TN and PA photoalignment," *Opt. Express* **20**(5), 5384–5391 (2012).
20. Y. Chen, J. Yan, J. Sun, S. T. Wu, X. Liang, S. H. Liu, P. J. Hsieh, K. L. Cheng, and J. W. Shiu, "A microsecond-response polymer-stabilized blue phase liquid crystal," *Appl. Phys. Lett.* **99**(20), 201105 (2011).
21. Z. Ge, S. Gauza, M. Jiao, H. Xianyu, and S. T. Wu, "Electro-optics of polymer-stabilized blue phase liquid crystal displays," *Appl. Phys. Lett.* **94**(10), 101104 (2009).
22. L. Rao, Z. Ge, S. Gauza, K. M. Chen, and S. T. Wu, "Emerging liquid crystal displays based on the Kerr effect," *Mol. Cryst. Liq. Cryst. (Phila. Pa.)* **527**(1), 30–42 (2010).
23. Y. Li and S. T. Wu, "Polarization independent adaptive microlens with a blue-phase liquid crystal," *Opt. Express* **19**(9), 8045–8050 (2011).
24. Y. H. Lin, H. S. Chen, H. C. Lin, Y. S. Tsou, H. K. Hsu, and W. Y. Li, "Polarizer-free and fast response microlens arrays using polymer-stabilized blue phase liquid crystals," *Appl. Phys. Lett.* **96**(11), 113505 (2010).
25. J. Yan, Y. Li, and S. T. Wu, "High-efficiency and fast-response tunable phase grating using a blue phase liquid crystal," *Opt. Lett.* **36**(8), 1404–1406 (2011).
26. G. Zhu, J. N. Li, X. W. Lin, H. F. Wang, W. Hu, Z. G. Zheng, H. Q. Cui, D. Shen, and Y. Q. Lu, "Polarization independent blue phase liquid crystal gratings driven by vertical electric field," *J. Soc. Inf. Disp.* **20**(6), 341–346 (2012).
27. J. L. Zhu, J. G. Lu, J. Qiang, E. W. Zhong, Z. C. Ye, Z. He, X. Guo, C. Y. Dong, Y. Su, and H. P. D. Shieh, "1D/2D switchable grating based on field-induced polymer stabilized blue phase liquid crystal," *J. Appl. Phys.* **111**(3), 033101 (2012).
28. J. Yan, Q. Li, and K. Hu, "Polarization independent blue phase liquid crystal gratings based on periodic polymer slices structure," *J. Appl. Phys.* **114**(15), 153104 (2013).
29. Z. G. Zheng, W. Hu, G. Zhu, M. Sun, D. Shen, and Y. Q. Lu, "Brief review of recent research on blue phase liquid crystal materials and devices," *Chin. Opt. Lett.* **11**(1), 011601–011605 (2013).
30. D. Luo, H. T. Dai, and X. W. Sun, "Polarization-independent electrically tunable/switchable Airy beam based on polymer-stabilized blue phase liquid crystal," *Opt. Express* **21**(25), 31318–31323 (2013).
31. A. V. Carpentier, H. Michinel, J. R. Salgueiro, and D. Olivieri, "Making optical vortices with computer-generated holograms," *Am. J. Phys.* **76**(10), 916–921 (2008).
32. H. Wu, W. Hu, H. C. Hu, X. W. Lin, G. Zhu, J. W. Choi, V. Chigrinov, and Y. Q. Lu, "Arbitrary photo-patterning in liquid crystal alignments using DMD based lithography system," *Opt. Express* **20**(15), 16684–16689 (2012).
33. G. Zhu, B. Y. Wei, L. Y. Shi, X. W. Lin, W. Hu, Z. D. Huang, and Y. Q. Lu, "A fast response variable optical attenuator based on blue phase liquid crystal," *Opt. Express* **21**(5), 5332–5337 (2013).
34. J. Yan, H. C. Cheng, S. Gauza, Y. Li, M. Jiao, L. Rao, and S. T. Wu, "Extended Kerr effect of polymer-stabilized blue-phase liquid crystals," *Appl. Phys. Lett.* **96**(7), 071105 (2010).
35. J. Yan and S. T. Wu, "Polymer-stabilized blue phase liquid crystals: a tutorial invited," *Opt. Mater. Express* **1**(8), 1527–1535 (2011).
36. C. Loussert, K. Kushnir, and E. Brasselet, "Q-plates micro-arrays for parallel processing of the photon orbital angular momentum," *Appl. Phys. Lett.* **105**(12), 121108 (2014).
37. X. Wang, M. Xu, H. Ren, and Q. Wang, "A polarization converter array using a twisted-azimuthal liquid crystal in cylindrical polymer cavities," *Opt. Express* **21**(13), 16222–16230 (2013).

## 1. Introduction

Optical vortices, which are characterized by helical wave fronts, have been studied extensively in the past two decades [1–3]. The number of phase windings in a single wavelength (defined as topological charge,  $m$ ) is a key parameter to describe these vortices. It determines the orbital angular momentum (OAM) of the beam [4] and adds a new degree of freedom to characterize the light properties, thus opening a door towards widespread applications in informatics, micro-manipulation, and astronomy [2, 5, 6]. Several techniques have been developed to generate optical vortices. In the initial research, Laguerre-Gaussian mode vortices were realized through cylindrical lens mode converters [4]. Subsequently, spiral phase plates were developed to generate optical vortices via directly rephasing plane waves [7, 8]. More recently, liquid crystals (LCs) have been introduced [9–11] to accomplish tunable vortex generators due to their excellent electro-optical (EO) properties. Typically, patterned electrodes [12], structured polymer dispersed LCs [13, 14] and photopatterned alignment layers [15] are used to prepare LC spiral phase plates or fork gratings for

generating switchable and reconfigurable optical vortices. “Fork” grating is a diffraction grating with dislocations in the center, which supplies a convenient approach for generating beam vortices [16, 17]. Q-plate, an inhomogeneously birefringent wave plate with specified geometry of the local optical axis, supports another option for vortex generation [9, 10]. The commercial spatial light modulator (SLM), which is usually a reflective liquid crystal display controlled by a computer, could generate arbitrary phase modulation including fork gratings and spiral phase plates [17].

Above LC techniques provide various available approaches for tunable vortex generation. However, the response of traditional nematic LCs is limited to tens of milliseconds [18, 19]. That drastically restricts the time for optical vortex switching and reconfiguring, which are essential to the performances of all these components. Therefore the exploiting of novel approaches for the realization of fast changing optical vortices is quite meaningful. The Kerr effect induced EO response of blue phase liquid crystals (BPLCs) can reach down to microsecond scale [20]. Besides fast response, BPLC also exhibits excellent features such as no requirement of alignment layers and optical isotropic voltage-off state. Thanks to the merits, BPLCs have been intensively studied in the field of both liquid crystal display [21, 22] and other optical fields, such as fast switchable lenses [23, 24], phase gratings [25–29] and cubic phase plates [30]. BPLC could also be a desired candidate for fast switchable optical vortex generator. In previous works, only a single converter can be created in one LC cell or one SLM [12, 17]. It would be difficult to prepare high quality converter arrays based on the above approaches. The reconfiguring of topological charge was accomplished through electrically refreshing the phase patterns or physically changing the generators. Very recently, Wei *et al.* realized high quality reconfiguration of  $m$  through photo rewriting the fork grating patterns [15]. All above strategies are time-consuming. To overcome the limit and process multiple beams simultaneously, one possible way is miniaturizing the aperture size of individual optical vortex generator and integrating a generator array in one cell.

In this work, a fast switchable optical vortex generator is demonstrated via a BPLC cell driven by vertical electric field with a forked electrode. This component can convert a Gaussian beam to diffracted vortex beams depend on the voltage generated forked phase profile. Moreover, an array of fork gratings with different  $m$  values is carried out, and fast beam steering technique could be employed to change the  $m$  through scanning different single fork gratings. This approach has great potentials in the fields of fast communication and micro-manipulation.

## 2. Principle and experiment

Specified computer-generated holograms can convert a Gaussian laser beam into desired helical modes. The helical wave front of an optical vortex can generally be described by the phase function  $\Psi_1 = \exp(im\theta)$ , where  $\theta$  is the azimuthal angle of a cylindrical coordinate system  $(r, \theta, z)$  around the  $z$  axis, which indicates the beam propagation direction, the topological charge  $m$  can be positive or negative, depending on the direction of the twist (positive for counterclockwise rotation and negative for clockwise rotation). To imprint a phase  $\Psi_1$  in a Gaussian beam, the interference of a reference tilted plane wave  $\Psi_2 = \exp(ikx)$  (where  $k$  is the spatial frequency indicating the tilting angle of the wave) and the object wave  $\Psi_1$  is utilized to form the computer-generated holograms. The interference pattern could be described by the function [31],

$$H = |\psi_1 + \psi_2|^2 = |\exp(im\theta) + \exp(ikx)|^2 = 2[1 + \cos(kx - m\theta)], \quad (1)$$

where  $\theta = \tan^{-1}(y/x)$ . Figure 1(a) shows the calculated computer-generated hologram plot of  $H$  for  $m = 1$ . The hologram pattern looks like a fork, with a branching in the central fringe. It carries information of the topological charge  $m$  and the reference wave.

Such holograms are transferred to photoresist by means of Digital Micro-mirror Device (DMD) based microlithography [32]. The DMD (Discovery 3000, Texas Instruments) consists of pixelated micro-mirrors, and each mirror can be independently tilted by an electrostatic force thus redirecting the reflected wave propagation. Here, it is used as a dynamic mask for generating arbitrary patterns including fork gratings. The exposed photoresist regions are developed and then the patterns are transferred to ITO layer through wet etching process. Through this method, high quality forked electrodes array can also be made easily by step by step exposure and one step etching. Finally, each patterned ITO glass is assembled with a bare ITO glass to form a cell. The cell gap is  $d = 12 \mu\text{m}$  controlled by Mylar films. As BPLC is to be filled, no rubbing process is needed, which simplifies the fabrication procedure.

The mixture of BPLC precursor (HCM-057, HCCH) and a small amount of photo initiator (IRG-184) was heated to an isotropic phase and then filled into the cell [33]. The sample was cooled at a cooling rate of  $0.2 \text{ }^\circ\text{C}/\text{min}$  with temperature precisely controlled by a heating and cooling stage (Linkam SLT 120) and observed under a transmission polarizing microscope (Nikon 50i) with orthogonal polarizers. A stable BP state was obtained at  $68^\circ\text{C}$ . We maintained the temperature and executed UV-curing at an intensity of  $5.3 \text{ mW}/\text{cm}^2$  for 8 minutes to stabilizing the precursor. After this procedure, a polymer-stabilized blue phase liquid crystal (PSBPLC) cell with forked electrodes was achieved.

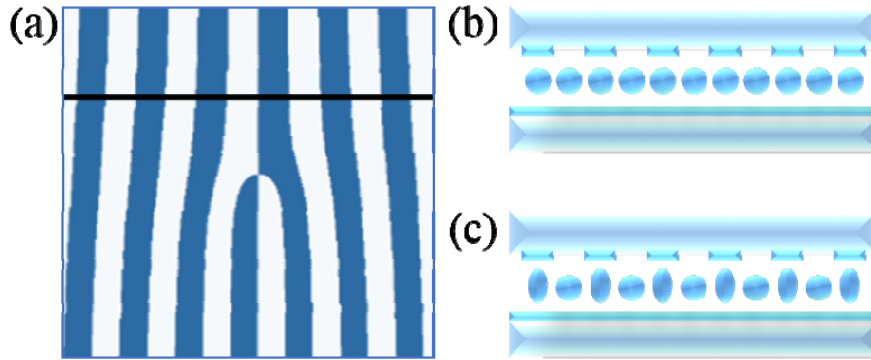


Fig. 1. (a) Schematic drawing of a fork grating electrode with  $m = 1$ , blue regions refer to the ITO. Refractive index distributions at the black line marked region in the forked PSBPLC cell with (b) no voltage applied and (c) voltage applied.

Generally, when no electric field is applied, the PSBPLC is uniformly optical isotropic (Fig. 1b). The refractive index is  $n_i = (2n_e + n_o)/3$ . When external field applied, the optical property of PSBPLC changes due to Kerr effect. As shown in Fig. 1(c), the refractive index to normally incident light in the electrode covered regions changes gradually from  $n_i$  to  $n_o$ , while that in the uncovered regions almost keeps  $n_i$  [26]. Thus the refractive index follows the changing of electrical field and forms a forked phase profile. In this case, the phase difference  $\Gamma$  between the two regions could be expressed by [34]

$$\Gamma = \frac{2\pi}{\lambda} [n_o(E) - n_i] d, \quad (2)$$

where  $\lambda$  is the wavelength,  $n_o(E)$  is the induced ordinary refractive index of PSBPLCs.

### 3. Results and discussions

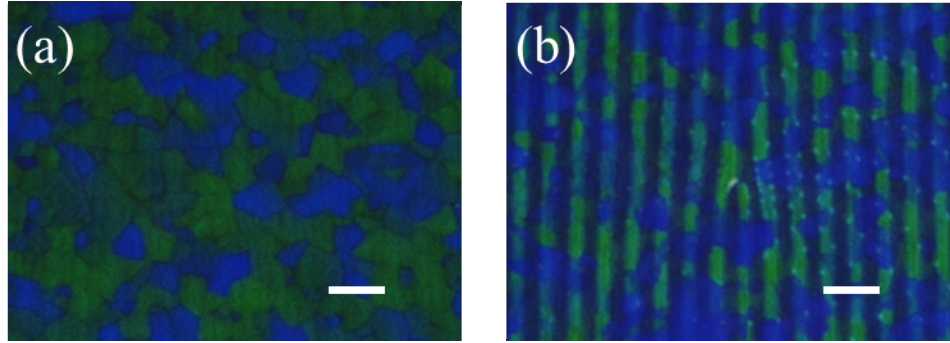


Fig. 2. Micrographs of PSBPLC cell taken with cross polarizers at (a) voltage-off state and (b) voltage-on state with  $80 V_{\text{rms}}$  applied. The scale bar is  $50 \mu\text{m}$ .

Figure 2(a) is a micrograph of the PSBPLC cell with  $m = 1$  forked electrode taken when no voltage is applied. As expected, uniform dark platelet textures were observed. The different color domains, which are in size of tens of micrometers, are due to the wavelength selective Bragg reflections of different orientated BPLC cubic lattices. As the cubic lattices are optically isotropic and their Kerr effects are independent on orientations, the non-uniform orientation here will not affect the EO properties [35]. Figure 2(b) reveals the same sample with  $80 V_{\text{rms}}$  applied. As we can see, a fork grating profile exactly the same as the patterned electrode is obviously revealed. The reason is the external field induced EO tuning of the PSBPLC. The transmittance at forked electrode covered regions increased, and that at uncovered regions keeps unchanged. A fork shaped phase profile with alternation of isotropic and ordinary refractive indices is thus obtained by applying a vertical electric field with a forked electrode, and a high quality fork grating is formed.

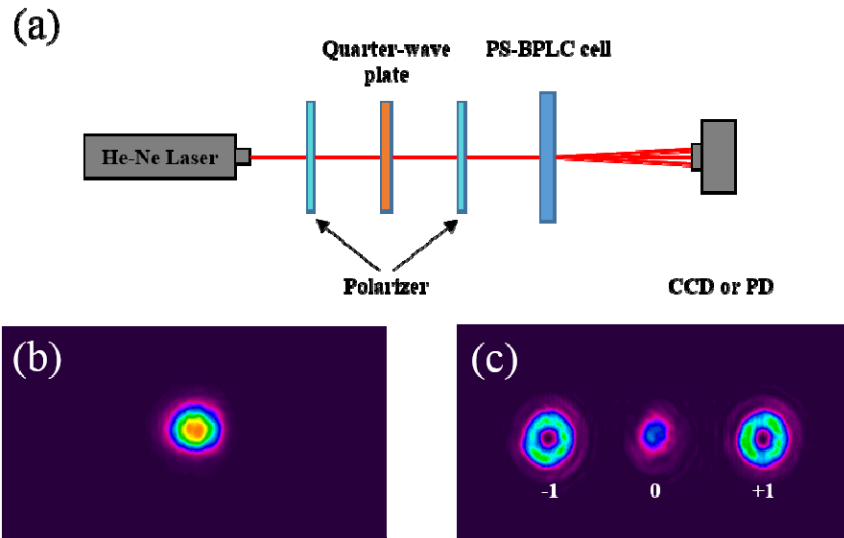


Fig. 3. (a) The vortex beam generation and detection setup and images of (b) off state and (c) on state of the optical vortex captured by a CCD.

The vortex beam generation and detection setup is schematically shown in Fig. 3(a). A laser beam from a He-Ne laser ( $632.8 \text{ nm}$ ) passes first through a polarizer and then a quarterwave plate ( $@633 \text{ nm}$ ) to generate a circular polarized light. Afterwards, it goes

through another polarizer and finally normally incidents to the sample. The quarter-wave plate and rear polarizer could be replaced by a single half-wave plate. The diffracted patterns are recorded by a CCD or received by a photodetector for the EO measurements. Figure 3(b) and 3(c) present the images of off state and on state of the optical vortex captured by a CCD respectively. At 0 V, only a Gaussian beam is observed as the PSBPLC is optical isotropic, the cell works as a uniform dielectric film. At voltage on state, 80 V<sub>rms</sub> for instance, optical vortices are observed in diffraction orders on both sides of order 0th. The topological charges of these optical vortices are given by  $nm$ , where  $n$  represents the diffraction order and  $m$  is the charge of the LC fork grating. Here, only the  $\pm 1$ st orders which are in highest efficiency are given. Thus a switch between on/off states could be easily accomplished via voltage control.

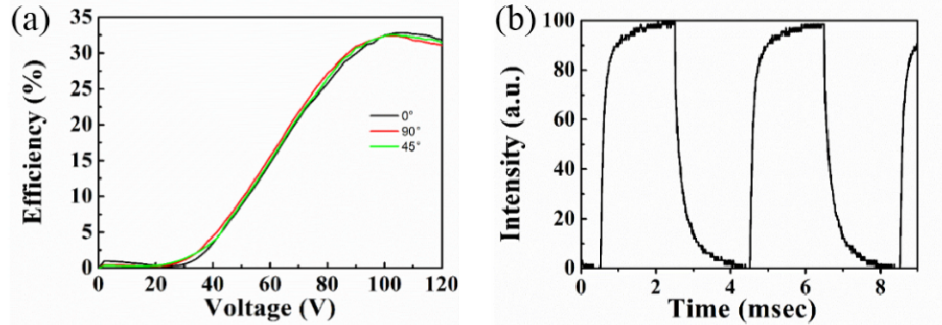


Fig. 4. (a) Polarization dependent  $V$ - $\eta$  curves of the 1st order optical vortex with  $0^\circ$ ,  $45^\circ$  and  $90^\circ$  incident polarizations. (b) EO response of the PSBPLC fork grating.

The polarization direction of incident beam could be freely tuned by simply rotating the second polarizer with a constant intensity. The voltage-dependent efficiency ( $V$ - $\eta$  curves) of the 1st order optical vortex at  $0^\circ$ ,  $45^\circ$  and  $90^\circ$  incident polarizations were measured separately and plotted in Fig. 4(a). Here, the efficiency is defined as the intensity ratio of the 1st diffraction order to the total transmittance at off state. The efficiency maximum occurs at  $\sim 95$  V<sub>rms</sub> when  $\Gamma$  reaches a  $\pi$ . The  $\eta$  ( $\sim 33\%$ ) is a little lower than the theoretical value ( $\sim 40\%$ ) of normal BPLC phase gratings [25]. The degradation may be assumed to the fringe field induced phase retardation. Despite of this, the efficiency is higher than traditional fork gratings, which are limited to 13–27% at present [12–14]. No obvious difference is observed between the two curves, implying a good polarization independency. The reason is that the forked phase profile is generated through the phase difference between  $n_i$  and  $n_o$ , both of which are independent on the normally incident laser beams [26]. The EO response of the PSBPLC fork grating is also tested. The switching on/off time here is defined as the duration that the intensity of the 1st order optical vortex changes from 10% to 90% and reverse. The measured switching on/off alternating between 0 V<sub>rms</sub> and 50 V<sub>rms</sub> are  $\tau_{\text{on}} = 364 \mu\text{s}$  and  $\tau_{\text{off}} = 571 \mu\text{s}$  respectively.

Shaping the phase of an optical field in realtime is a common requirement for many applications, such as space-division multiplexing of the OAM of light. However, instantly reconfiguring the topology of light fields and the realization of efficient parallel processing of OAM at small scale remain challenges. The development of beam converter arrays is considered a practical strategy [36, 37], while in practice, state-of-the-art fabricating of miniaturized optical mode converters array is not so easy to date. Here, we employed the DMD based lithography, the well-established technique for high quality micro fabrications, to carry out the forked electrodes array. Thanks to the excellent generating flexibility and splicing capability of the system, the required PSBPLC fork grating array is achieved as exhibited in Fig. 5. Fork gratings with  $m$  from 1 to 4 are demonstrated. At voltage-on state, the optical contrast reveals good replica of corresponding electrode. Through this technique, larger  $m$  values and larger arrays are both achievable. Combined with fast beam steering

technique, rapid changing among different OAM is possible. Therefore arbitrary coding, even multiplexing and demultiplexing of OAM could be accomplished, which is of great significance in OAM based informatics and micro-manipulations.

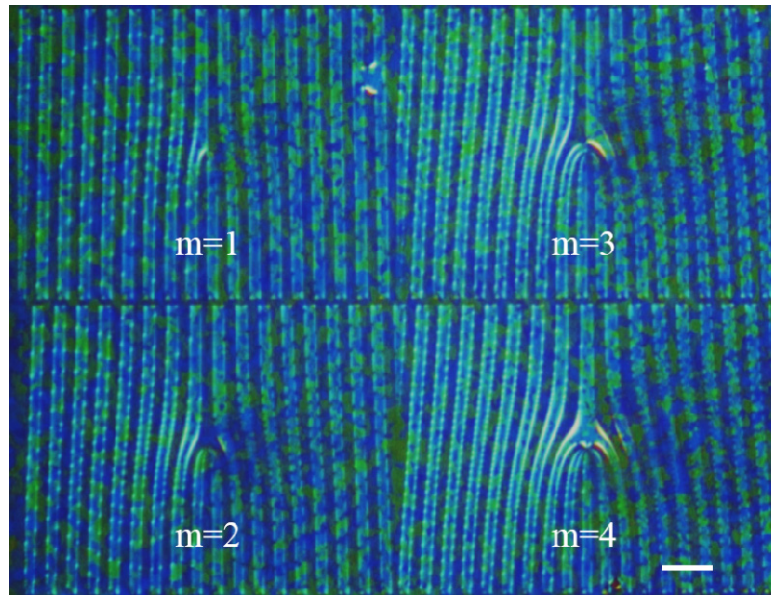


Fig. 5. Micrograph of a PSBPLC fork grating array with  $m$  varying from 1 to 4 at  $80 V_{rms}$ . The scale bar is  $100 \mu m$ .

#### 4. Conclusion

In this work, vortex beam generators based on PSBPLC fork gratings are demonstrated. The phase profile is formed by the alternation of isotropic and vertical field induced ordinary refractive index. The samples can convert Gaussian beams to vortex beams efficiently. Advantages such as simplified fabrication procedure, fast electrical tunability/switchability and polarization independency are exhibited. Through this strategy, multi-generator can be created in a single LC cell, thus topological charge can be rapidly tuned through beam steering. The proposed design is quite suitable for preparing high quality miniaturized optical vortex generators and generator arrays, and has great potentials in informatics, micro-manipulation, and astronomy.

#### Acknowledgments

This work is sponsored by 973 programs (Nos. 2011CBA00200 and 2012CB921803), the National Natural Science Foundation of China (Nos. 11304151, 61435008) and Ph.D. Programs Foundation of Ministry of Education of China (No. 20120091120020).